

82-11-27

DEUTSCHES ELEKTRONEN-SYNCHROTRON **DESY**

DESY 82-064
September 1982

EXPERIMENTAL STUDY OF THE PHOTON STRUCTURE FUNCTION F_2
IN THE HIGH Q^2 REGION

by

JADE Collaboration

NOTKESTRASSE 85 · 2 HAMBURG 52

DESY behält sich alle Rechte für den Fall der Schutzrechtserteilung und für die wirtschaftliche Verwertung der in diesem Bericht enthaltenen Informationen vor.

DESY reserves all rights for commercial use of information included in this report, especially in case of filing application for or grant of patents.

**To be sure that your preprints are promptly included in the
HIGH ENERGY PHYSICS INDEX,
send them to the following address (if possible by air mail) :**

**DESY
Bibliothek
Notkestrasse 85
2 Hamburg 52
Germany**

Experimental study of the photon structure function F_2 in the high Q^2 region.

JADE Collaboration

W. Bartel, D. Cords, G. Dietrich, P. Dittmann¹, R. Eichler², R. Felst, D. Haidt, H. Krehbiel, K. Meier, B. Naroska, J. Olsson, L.H. O'Neill³, P. Steffen
Deutsches Elektronen-Synchrotron DESY, Hamburg, Germany

E. Elsen, A. Petersen, P. Warming, G. Weber

II. Institut für Experimentalphysik der Universität Hamburg, Germany

S. Bethke, J. Heintze, G. Heinzelmann, K.H. Hellenbrand, R.D. Heuer, J. von Krogh, P. Lennert, S. Kawabata⁴, S. Komamiya, H. Matsumura, T. Nozaki, H. Rieseberg, A. Wagner
Physikalisches Institut der Universität Heidelberg, Germany

A. Bell, F. Foster, G. Hughes, H. Wriedt

University of Lancaster, England

J. Allison, A.H. Ball, G. Bamford, R. Barlow, C. Bowdery, I.P. Duerdoth, I. Glendinning, F.K. Loebinger, A.A. Macbeth, H. McCann, H.E. Mills, P.C. Murphy, P. Rowe, K. Stephens
University of Manchester, England

D. Clarke, M.C. Goddard, R. Marshall, G.F. Pearce,

Rutherford Appleton Laboratory, Chilton, England

J. Kanzaki, T. Kobayashi, M. Koshiha, M. Minowa, M. Nozaki, S. Odaka, S. Orito, A. Sato, H. Takeda, Y. Totsuka, Y. Watanabe⁵, S. Yamada, C. Yanagisawa⁵

Lab. of Int. Coll. on Elementary Particle Physics and Department of Physics, University of Tokyo, Japan

¹Deceased

²Now at Labor. f. Hochenergiephysik der ETH-Zürich, Villigen, Switzerland

³Now at Bell Laboratories, Whippany, N.J., U.S.A.

⁴Now at KEK, Oho-Machi, Tsukuba-Gun, Ibaraki-Ken, Japan

⁵Now at Rutherford Appleton Laboratory, Chilton, England

Abstract:

We report on a measurement of the process $e^+ e^- \rightarrow e^+ e^- + \text{hadrons}$, where one of the scattered electron is detected at large angles, with an average Q^2 of 23 GeV². The results are analysed in terms of the photon structure function F_2 and are compared with QCD predictions.

Deep inelastic electron photon scattering,

$$e^+ \gamma \rightarrow e^+ + \text{hadrons} \quad (1)$$

provides a good test of Quantum Chromodynamics, QCD. The cross section is believed to be dominated by the pointlike contribution at high Q^2 (four momentum transfer squared), which can be calculated by perturbative QCD⁽¹⁾. The measurement of the two photon initiated hadron production,

$$e^+ e^- \rightarrow e^+ e^- + \text{hadrons} \quad (2)$$

provides an opportunity to study reaction (1) if one of the scattered electrons is detected at a large angle while the other electron is scattered under small angles, which is usually the case if it is not detected (single tag condition)^(2,3). The basic diagram of reaction (2) is shown in Fig.(1a).

Under the single tag condition, the cross section of reaction (2) is given, to a good approximation, by the cross section of reaction (1), multiplied by a flux factor of quasi real photons $N(z, \Theta_{2\text{max}})$ ⁽⁴⁾,

$$\sigma(ee \rightarrow ee+X) = \int \sigma(e^+ \gamma \rightarrow e^+ X) N(z, \Theta_{2\text{max}}) dz \quad (3)$$

The function $N(z, \Theta_{2\text{max}})$, which provides the number of quasi real photons per dz , is obtained from the equivalent photon approximation^(4,5),

$$N(z, \Theta_{2\text{max}}) = \alpha / (\pi z) \{ [1 + (1-z)^2] \ln \{ (E/m_e) ((1-z)/z) \Theta_{2\text{max}} \} - 1 + z \} \quad (4)$$

with $z = E_\gamma/E$, E = beam energy, E_γ = energy of quasi real photon, $\Theta_{2\text{max}}$ = the maximum scattering angle of the undetected electron and m_e the electron mass.

In terms of the photon structure functions F_2 and F_L the cross section of deep inelastic electron photon scattering is given by⁽⁴⁾

$$d\sigma/dE d(\cos\theta) = (4\pi\alpha^2 E' / (Q^4 y)) \{ (1 + (1-y)^2) F_2(x, Q^2) - (2xy^2) F_L(y) \} \quad (5)$$

Q^2 and the scaling variables x and y are given by: $Q^2 = 4 E E' \sin^2(\theta/2)$, $x = Q^2 / (Q^2 + W^2)$ and $y = 1 - (E'/E) \cos^2(\theta/2)$, where E' and θ are the energy and the polar angle of the tagged electron, respectively, and W is the total CM energy of the produced hadron system. The second term of eq.(5) is much smaller than the first one, since the average y^2 in this experiment is about 0.07 due to the selection criteria described below. Also QCD predicts the value of F_2 to be smaller than that of F_2 in the Q^2 region of the present experiment. The term F_2 is therefore neglected in the analysis. A first experimental analysis of this sort at $\langle Q^2 \rangle = 5 \text{ GeV}^2$ was reported by the PLUTO Collaboration (6).

The data of the present analysis have been taken with the JADE detector at the e^+e^- colliding beam facility PETRA. The JADE detector has been described elsewhere (7) and here we mention only those features which were essential for this analysis. The tagging of the electrons was carried out using the two arrays of endcap lead glass counters which cover the angular range from 245 to 500 mrad with respect to the beams. Charged tracks were detected with the central drift chamber (jet chamber) (8) covering 97% of the solid angle and situated in a magnetic field of 4.8 kG. Photons and electrons were detected in the lead glass shower counters, covering 90% of the solid angle.

The hadronic two photon events of reaction (2) were selected by applying the following criteria:

a) The detection of an electron is required in one of the two arrays of endcap lead glass counters with an energy exceeding $0.5 E_{\text{beam}}$. In order to remove the effects of the counter edges, the angular range of the tagged electron was restricted to $\theta = 265-428 \text{ mrad}$. These selection criteria yield Q^2 values ranging from 10 to 60 GeV^2 , on average $\langle Q^2 \rangle = 23 \text{ GeV}^2$. In addition, a track in the central chamber with at least 10 hits had to be associated with the tagged lead glass cluster. b) The absence of a second high energy electron with an energy in excess of $0.25 E_{\text{beam}}$ elsewhere in the whole lead glass arrays was required. c) Only events with $W_{\text{vis}} > 1 \text{ GeV}$ were accepted. Here W_{vis} is the visible CM energy of the produced hadron system and is calculated by means of the measured momenta of charged tracks and photons assuming pion masses for all charged tracks. d) At least three additional charged tracks or two additional charged tracks plus at least one photon were demanded. The charged tracks were required to have transverse momentum $> 0.1 \text{ GeV}/c$ and $\cos\theta_1 < 0.970$ where θ_1 is the polar angle of the track with respect to the beam line. Tracks due to converted photons were not included. Photons were detected as clusters in the barrel- and endcap lead glass counters and were required to have energies larger than 0.1 GeV and $\cos\theta_1$,

< 0.970 , with θ_1 the polar angle of the photon. The cuts b) and d) suppressed the dominant background originating from the QED processes $e^+e^- \rightarrow e^+e^-$, $e^+e^- \rightarrow e^+e^-e^+e^-$, $e^+e^- \rightarrow e^+e^-\mu^+\mu^-$ and their higher order contributions like $e^+e^- \rightarrow e^+e^-\gamma$, to a level of about 10% of the selected events. QED processes which could not be excluded by these cuts either contained hard photons or produced electromagnetic showers in the materials in front of the central chamber. These events were finally rejected by scanning all the remaining events and using the dE/dx , lead glass and muon chamber information. e) 1γ annihilation events containing hard photons radiated from the initial state constitute a background to reaction (2) because the probability for the photon emitted into the tagging angular range to convert into a e^+e^- pair is on the average 40%. The resulting e^+e^- pair usually looks like a single short track thus imitating a tagged electron. On the other hand 1γ annihilation events have much smaller longitudinal momentum balance (LMB) than 2γ hadronic events. LMB is defined as: $\text{LMB} = (\cos\theta / \cos\theta_1) \sum p_{i\parallel} \cos\theta_i$, where the sum is over both charged tracks and photons as well as over the tagged electron and θ is the polar angle of the tagged electron. Therefore the event was rejected if the tagged track had a dE/dx value larger than one standard deviation away from that expected for a single electron, where dE/dx was measured in the jet chamber (9), and in addition LMB was smaller than 7.5 GeV/c . Monte Carlo calculations (9,10) show that about 55% of the 1γ annihilation events imitating reaction (2) were rejected by these cuts while only about 2% of events from the reaction (2) are lost with these cuts.

176 events survived these cuts for an integrated luminosity of 20.2 pb^{-1} at an average beam energy of 16.8 GeV .

These events were corrected for the following remaining background contributions: 1) $e^+e^- \rightarrow e^+e^-\tau^+\tau^-$: This background was calculated using Monte Carlo techniques and the number of events was found to be 25 ± 2.5 . 2) $e^+e^- \rightarrow \tau^+\tau^-$: 4.6 ± 1.6 background events were obtained using Monte Carlo estimates. 3) Inelastic Compton scattering (Fig.(1b)): This background was calculated using the cross section formula given in ref.(1) and the resulting number was 4.1 ± 0.3 events. 4) Beam gas events: From the vertex distribution along the beam line a background of 3.8 ± 1.1 events was estimated. 5) Hadronic 1γ annihilation events with initial radiation: The number of remaining annihilation events was estimated to be 14 ± 5.5 from a comparison of the observed LMB distributions at small LMB with model calculations for 2γ production (10) and 1γ annihilation (9). After subtraction of these background contributions, 125 ± 15 events remained. The errors quoted above are statistical only.

In order to compare these data with various theoretical predictions, the x_{vis} distribution was calculated, with $x_{vis} = Q^2 / (Q^2 + W_{vis}^2)$. W_{vis} is on the average 30% smaller than the true W due to the loss of particles outside the limited acceptance. Thus x_{vis} is normally larger than the true x . Q^2 is calculated from the measured energy and polar angle of the scattered electron. The x_{vis} distributions from the various background sources have been estimated using Monte Carlo techniques except for the beam gas events where the real data with different vertex cuts were used. These distributions have been subtracted from the data bin by bin. The resulting x_{vis} distribution is shown in Fig.(2) (11).

Fig.(2) also contains several theoretical predictions resulting from a computer simulation of reaction (2) in the JADE detector. In this simulation first $e^+e^- \rightarrow e^+e^-q\bar{q}$ events were produced (10) according to eq.(3),(4) and (5) using the $F_2(x, Q^2)$ functions discussed below. The hadronic part of F_2 , which arises from a vector meson like component of the photon, was neglected since the hadronic part of F_2 is expected to be small at high Q^2 and to contribute mainly in the small $x(x_{vis})$ region (1). The quark masses were assumed to be: $m_u = m_d = 300 \text{ MeV}/c^2$, $m_s = 500 \text{ MeV}/c^2$ and $m_c = 1.6 \text{ GeV}/c^2$. For this calculation the photon flux given by eq.(4) was slightly modified, since it is not accurate enough for $\Theta_{max} = 245 \text{ mrad}$ as given by the acceptance of the endcap lead glass counters. For this renormalisation an exact calculation of the process $ee \rightarrow eeq$ (12) was used. In the second step the quarks were fragmented via the standard Field Feynman fragmentation scheme (13). We used the same parameters as employed in our previous analysis of high p_t jets from two photon interactions (14). In the third step the resolution of the jet chamber and lead glass counters was included. The electron showers in the endcap lead glass counters were simulated by means of a Monte Carlo program for three dimensional electro-magnetic shower development in lead glass (15). In the fourth step the Monte Carlo events were passed through the same analysis programs which were used for the analysis of the real data. Nuclear interactions of charged tracks in the materials in front of the chamber were taken into account. This Monte Carlo simulation of reaction (2) reproduced various observed distributions like multiplicity and momentum distributions of charged particles and photons, the Q^2 distribution of tagged electrons and the W_{vis} distribution of the produced hadron system rather well.

The following structure functions $F_2(x, Q^2)$ have been used as input for these calculations:

a) The quark parton model function (QPM)

$$F_2(x, Q^2, \text{QPM}) = (3\alpha/\pi) \sum_{i=u,d,s,c} e_i^4 \{ x(x^2 + (1-x)^2) \ln(W^2/m_{c,q}^2) + 8x^2(1-x) - x \} \quad (6)$$

where e_i = quark charge, $m_{c,q}$ = quark mass and $W^2 = Q^2(1/x - 1)$. Note that because of the high W^2 , contributions from the c quark have to be included. For the c quark we actually used a more lengthy formula without approximation of the light quark masses (16).

b) Leading order QCD (LOQCD)

$$F_2(x, Q^2, \text{LOQCD}) = (3\alpha/\pi) \sum_{i=u,d,s,c} e_i^4 f(x, \text{LOQCD}) \ln(Q^2/\Lambda^2) \quad (7)$$

which includes QCD corrections in leading order. Λ_{LO} is the QCD scale parameter in leading order approximation. Several authors have calculated $f(x, \text{LOQCD})$ by different methods and obtained similar results (17,18,19,20). The results of ref.(17) were used in the present analysis. Since no QCD calculations exist which include quark mass effects, we had to use the same F_2 for all flavours. Only phase space effects were taken into account by setting F_2 to zero for the c quark in the range $x > x_{th}$. ($x_{th} = Q^2 / (Q^2 + 4m_c^2)$).

c) Higher order QCD (HOQCD)

$$F_2(x, Q^2, \text{HOQCD}) = (3\alpha/\pi) \sum_{i=u,d,s,c} e_i^4 \{ f(x, \text{LOQCD}) \ln(Q^2/\Lambda^2) + g(x) \ln(\ln(Q^2/\Lambda^2 \bar{M}_S)) + h(x) \} \quad (8)$$

which includes recent QCD calculations in next to leading order (21,22,23). \bar{M}_S is the QCD scale parameter in the \bar{M}_S scheme (24). We numerically determined the functions $f(x, \text{LOQCD})$, $g(x)$ and $h(x)$ from the results given in ref.(23) and computed $F_2(x, Q^2, \text{HOQCD})$ using eq.(8). The contribution from the small x region where F_2 becomes negative was neglected in the Monte Carlo simulation of the x_{vis} distribution (23). The same treatment of the c quark was done as for b).

The resulting x_{vis} distributions are shown in Fig.(2a)-(2c). Fig.(2a) shows the quark parton model (QPM) prediction together with the leading order (LOQCD) and higher order QCD (HOQCD) predictions both for $\Lambda = 0.3 \text{ GeV}$. All three curves provide a reasonable description of data with the exception of the lowest x_{vis} -bin, reflecting a reasonable choice of the quark masses in eq.(6) and of the QCD parameter Λ in eq.(7) and (8). The curves of Fig.(2) are quite sensitive to the parameter Λ as indicated in Fig.(2b), and in principle allow its determination. These QCD calculations, however, neglect quark mass effects (except for the phase space effect mentioned above), an approximation not justified for the c quark. The uncertainties introduced by the treatment of the c quark can be estimated from Fig.(2c) where the leading order QCD predictions are shown with and without the c quark contribution. Also shown is a curve for which the light quark (u, d, s) contribution was calculated by LOQCD but the c quark contribution was calculated by the QPM. The QCD parameter Λ obtained by fitting the data

with the theoretical predictions in the region of $x_{vis} > 0.4$ are listed in table 1. These values are consistent with values of $\Lambda_{10} \sim \Lambda_{\overline{MS}} = 0.1$ to 0.35 GeV obtained from deep inelastic lepton nucleon scattering experiments (28).

LOQCD as well as QPM predict the $\ln(Q^2)$ dependence of the photon structure function of F_2 for fixed x . Fig.(3) shows the Q^2 dependence of the function $F_2(x, Q^2)$ averaged over the range $x_{vis} > 0.3$, where the correlation between Q^2 and x is found to be small according to Monte Carlo calculations. Also shown in Fig.(3) are the results of a similar analysis at smaller Q^2 by the PLUTO Collaboration(6). For comparison the LOQCD prediction is shown for $\Lambda_{10} = 0.3$ GeV. The LOQCD prediction without the c quark contribution is separately indicated. It is seen that, while the JADE data are consistent with the LOQCD prediction the lower Q^2 PLUTO points are located above these curves. This might be due to the hadronic contribution to F_2 which is expected to be more significant in the PLUTO data because of the smaller Q^2 (1,6).

In summary, a measurement of the process $e^+ e^- \rightarrow e^+ e^- +$ hadrons was carried out under the single tag condition at an average Q^2 of 23 GeV². The results were analysed in terms of the photon structure function F_2 and they were found to be well described by leading order QCD in the whole x_{vis} region. Also quark parton model as well as higher order QCD predictions agree well with the data except in the small x_{vis} region. The QCD parameter Λ was determined to $\Lambda_{\overline{MS}} = 0.18 (+0.12, -0.07)$ GeV if higher order corrections are taken into account and if the c-quark contribution is taken from the quark parton model. Future improvements demand not only higher statistics but also a proper treatment of heavy quarks in the perturbative QCD calculations.

We are indebted to the PETRA machine group for their excellent support and to all the engineers and technicians who have participated in the construction and maintenance of the apparatus. This experiment was supported by the UK Science Research Council through the Rutherford Laboratory, by the Educational Ministry of Japan and by the Bundesministerium für Forschung und Technologie. The visiting groups wish to thank the DESY directorate for their hospitality.

Table Caption

1. Measured values of Λ_{10} and $\Lambda_{\overline{MS}}$ for three different models.

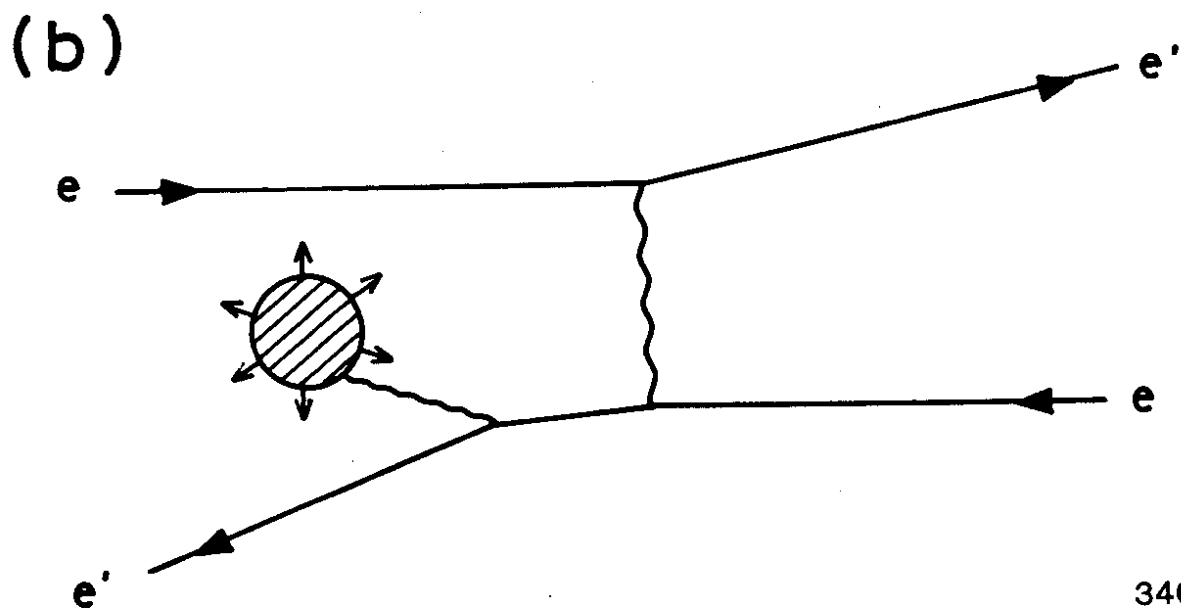
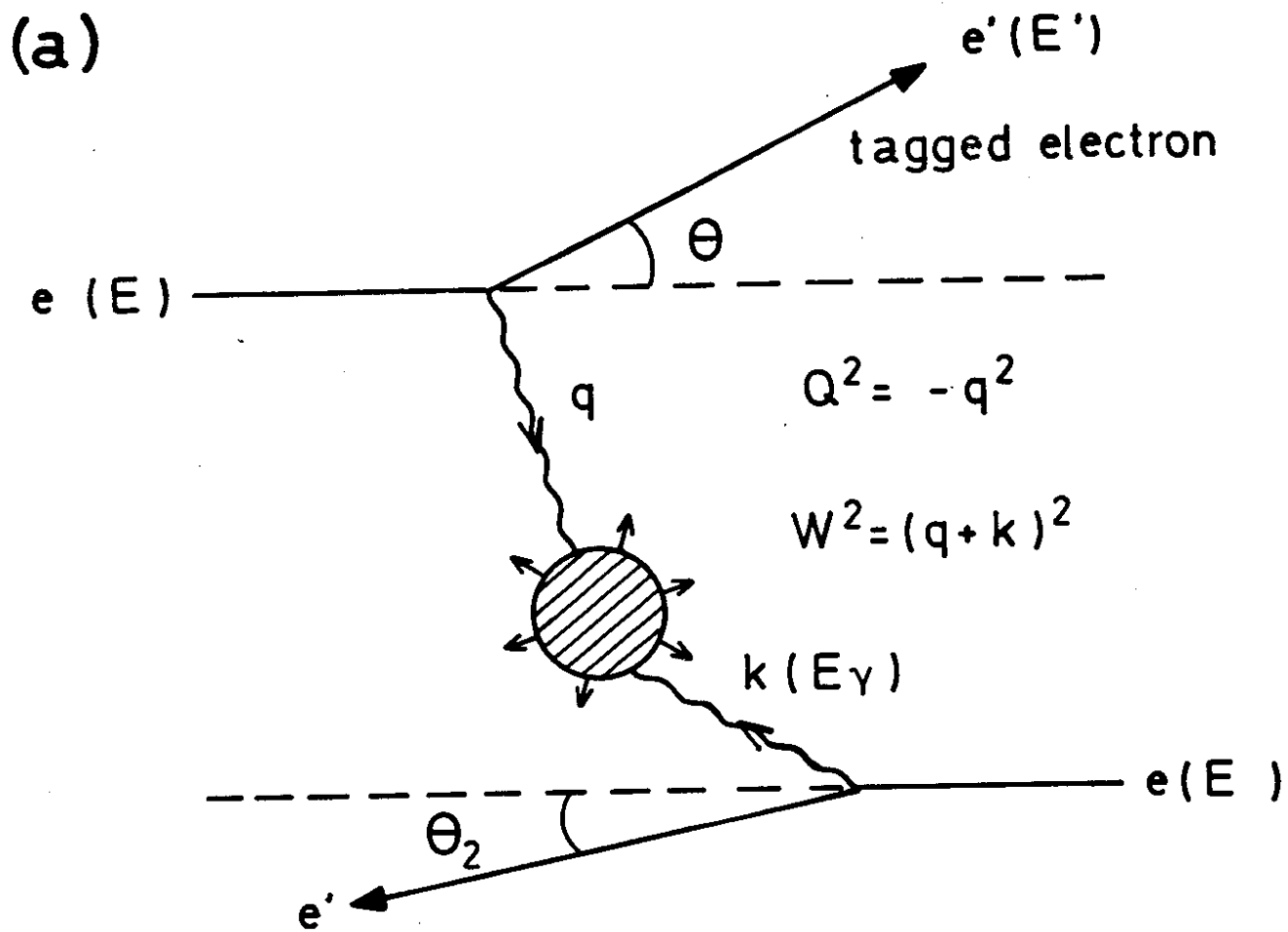
Figure Captions

1. a) Feynman diagram of $e^+e^- \rightarrow e^+e^- +$ hadrons.
b) Feynman diagram of inelastic Compton scattering.
 2. a) x_{vis} distribution. Solid curve = LOQCD (u, d, s, c) with $\Lambda_{10} = 0.3$ GeV. Dash-dotted curve = HOQCD (u, d, s, c) with $\Lambda_{\overline{MS}} = 0.3$ GeV. Dashed curve = QPM (u, d, s, c)
b) x_{vis} distribution. Solid curves = LOQCD (u, d, s, c) with $\Lambda_{10} = 0.1$ and 0.4 GeV. Dashed curves = HOQCD (u, d, s, c) with $\Lambda_{\overline{MS}} = 0.1$ and 0.4 GeV.
c) x_{vis} distribution. Solid curve = LOQCD (u, d, s, c) with $\Lambda_{10} = 0.3$ GeV. Dash-dotted curve = LOQCD (u, d, s) with $\Lambda_{10} = 0.3$ GeV plus QPM(c). Dashed curve = LOQCD (u, d, s) with $\Lambda_{10} = 0.3$ GeV.
 3. F_2/α as a function of Q^2 . Full circles(JADE data) = $F_2(x, Q^2)/\alpha$ averaged over $x_{vis} > 0.3$. Open circles(PLUTO data) = $F_2(x, Q^2)/\alpha$ averaged over $0.2 < x_{vis} < 0.8$. Solid curve = LOQCD (u, d, s, c) with $\Lambda_{10} = 0.3$ GeV. Dashed curve = LOQCD (u, d, s) with $\Lambda_{10} = 0.3$ GeV.
- #### References
1. C.Petersen, T.F.Walsh and P.M.Zerwas, Nucl.Phys. B174(1980)424.
 2. S.J.Brodsky, T.Kinoshita and H.Terazawa, Phys.Rev.D4(1971)1532.
 3. T.F.Walsh. Phys.Lett. 36B(1971)121.
 4. V.M.Budnev et al., Phys.Rep. 15C(1975)182.
 5. C.Carimalo, P.Kessler and J.Parisi, Phys.Rev. D21(1980)669.
 6. PLUTO Collaboration, Ch.Berger et al., Phys.Lett. 107B(1981)168.
 7. JADE Collaboration, W.Bartel et al., Phys.Lett. 88B(1979)171. ibid., 92B(1980)206 and 99B(1981)277.
 8. H.Drumm et al., Nucl. Inst. and Meth., 176(1980)333. J.Heintze, Nucl. Inst. and Meth., 196(1982)293. A.Wagner, Proc. of the Int. Conf. on Instrumentation for Colliding Beam Physics, SLAC 1982, SLAC-Report 250,p76.
 9. B.Andersson, G.Gustafson, T.Sjöstrand, Phys.Lett. 94B(1980)211, T.Sjöstrand, LUTP 80-3 (April 1980) and Errata to LUTP 80-3.
 10. S.Kawabata, Program Write-Up(1982), unpublished.

11. Preliminary results of this experiment were reported at the XVIIIth Rencontre De Moriond, Les Arcs-Savoie-France, March, 1982. In the old analysis the τ background was not corrected for and also the absence of c quark contributions in the high x region was not properly taken into account in the plot of $c' F_2(x, Q^2)$.
12. P Bhattacharya, J. Smith and G. Grammer, Phys. Rev. D15(1977)3267.
J. Smith, J. A. M. Vermaseren and G. Grammer, Phys. Rev. D15(1977)3280.
J. A. M. Vermaseren, Program Write-Up (1978), unpublished.
13. R. D. Field and R. P. Feynman, Nucl. Phys. B136(1978)1.
14. JADE Collaboration, W. Bartel et al., Phys. Lett. 107B(1981)163.
15. A. Sato, Master Thesis, University of Tokyo, 1978, unpublished.
K. Messel and J. F. Crawford, Electron-photon shower distribution function tables (Pergamon, London, 1970)
16. C. T. Hill and G. G. Ross, Nucl. Phys. B148(1979)373.
17. E. Witten, Nucl. Phys. B120(1977)189.
18. C. H. Llewellyn Smith, Phys. Lett. 79B(1978)83.
19. W. E. Frazer and J. Gunion, Phys. Rev. D20(1979)147.
20. R. J. Dewitt et al., Phys. Rev. D19(1979)2046.
21. W. A. Bardeen and A. J. Buras, Phys. Rev. D20(1979)166.
22. D. W. Duke and J. F. Owens, Phys. Rev. D22(1980)2280.
23. T. Uematsu and T. F. Walsh, Fermilab-PUB-81/55-THY.
24. W. A. Bardeen et al., Phys. Rev. D18(1978)3998.
25. The negative value of F_2 in the small x region which is predicted by HQCD might be compensated by the additional hadronic component of F_2 . See ref.(23) and W. A. Bardeen, Proc. of the 1981 Int. Symp. on Lepton and Photon Interactions at High Energies, Bonn 1981, p.432.
26. J. Katschack, Proc. of the 1981 Int. Symp. on Lepton and Photon Interactions at High Energies, Bonn 1981, p.461. J. Drees, ibid., p.474.
F. Eisele, Proc. of Xth Int. Winter Meeting on Fundamental Physics and

Table 1

	Λ_{LO}	Λ_{MS}
QCD (udsc)	$0.28^{+0.13}_{-0.09}$ GeV	$0.22^{+0.10}_{-0.07}$ GeV
QCD (uds)+QPM(c)	$0.21^{+0.17}_{-0.09}$ GeV	$0.18^{+0.12}_{-0.07}$ GeV
QCD (uds)	$0.07^{+0.05}_{-0.03}$ GeV	$0.06^{+0.05}_{-0.03}$ GeV



34608

Fig. 1

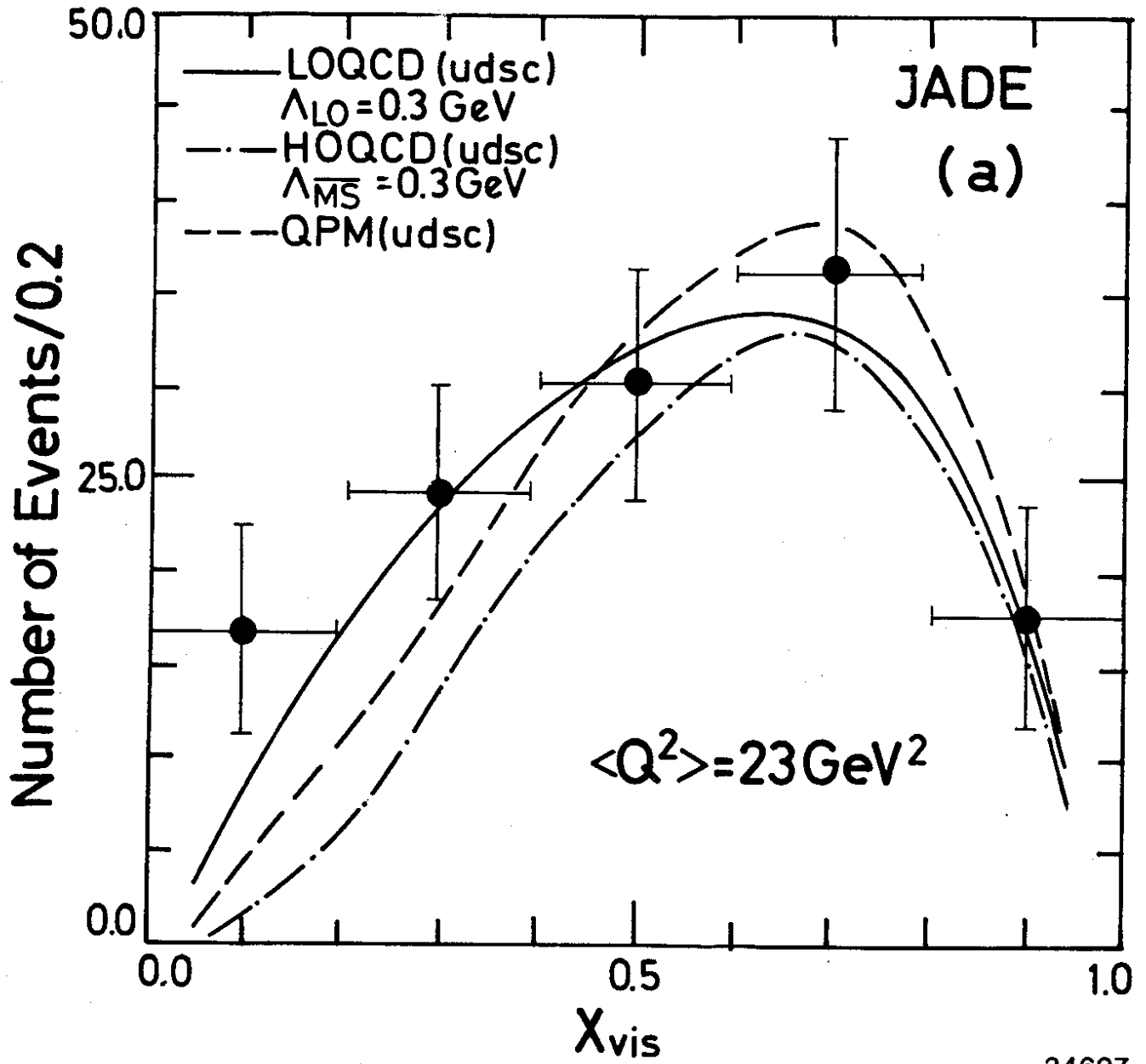


Fig. 2a

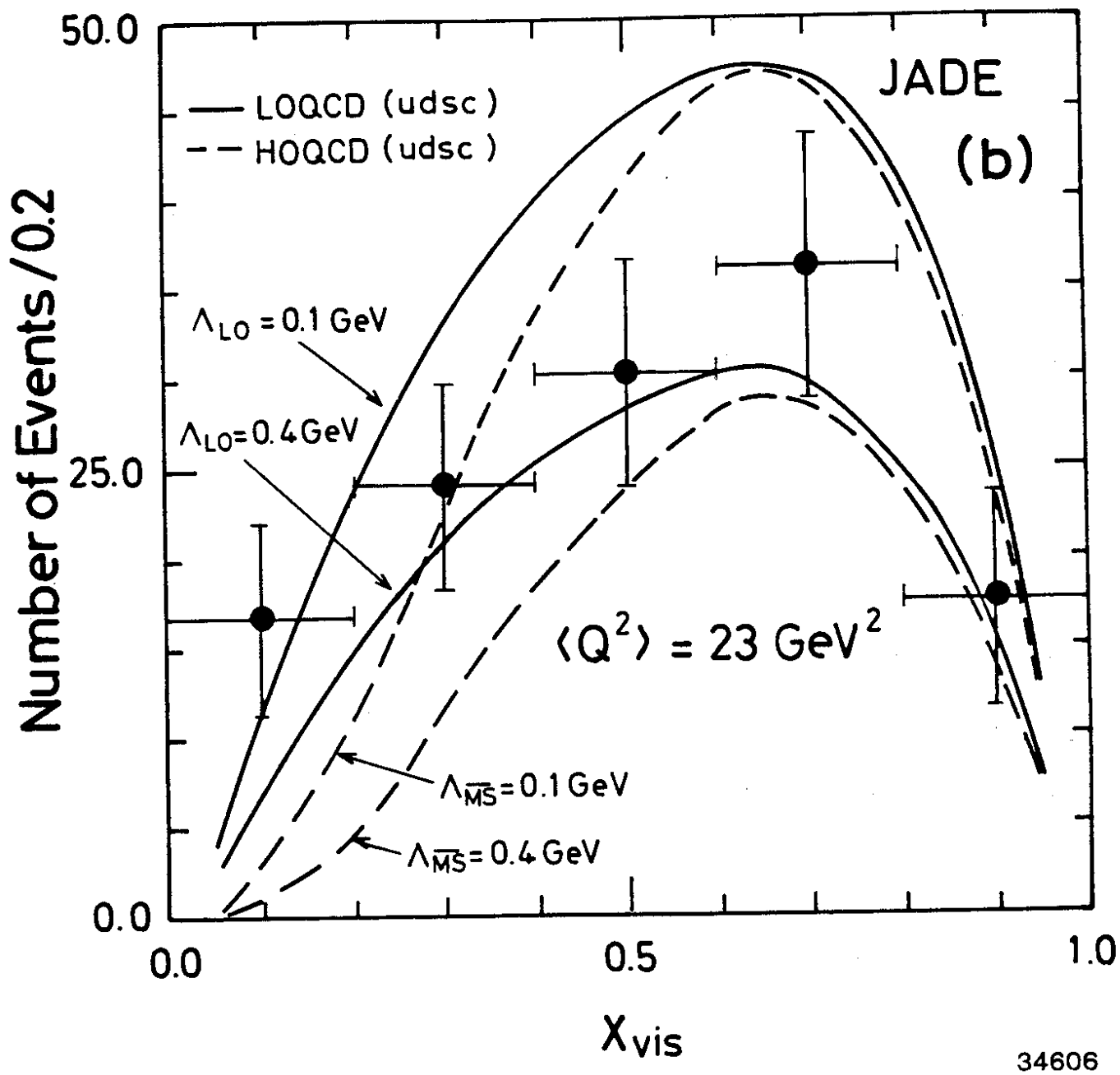
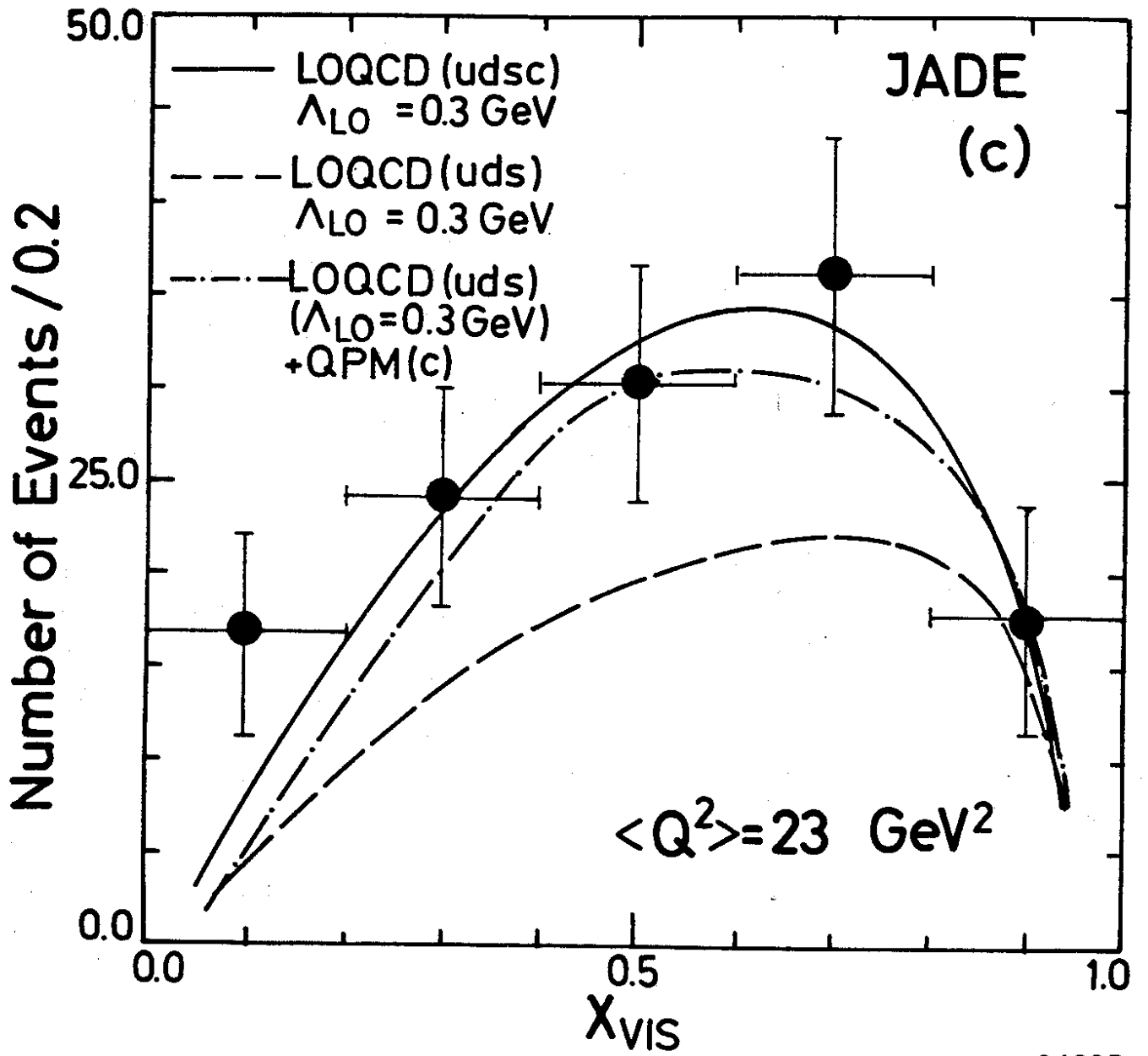
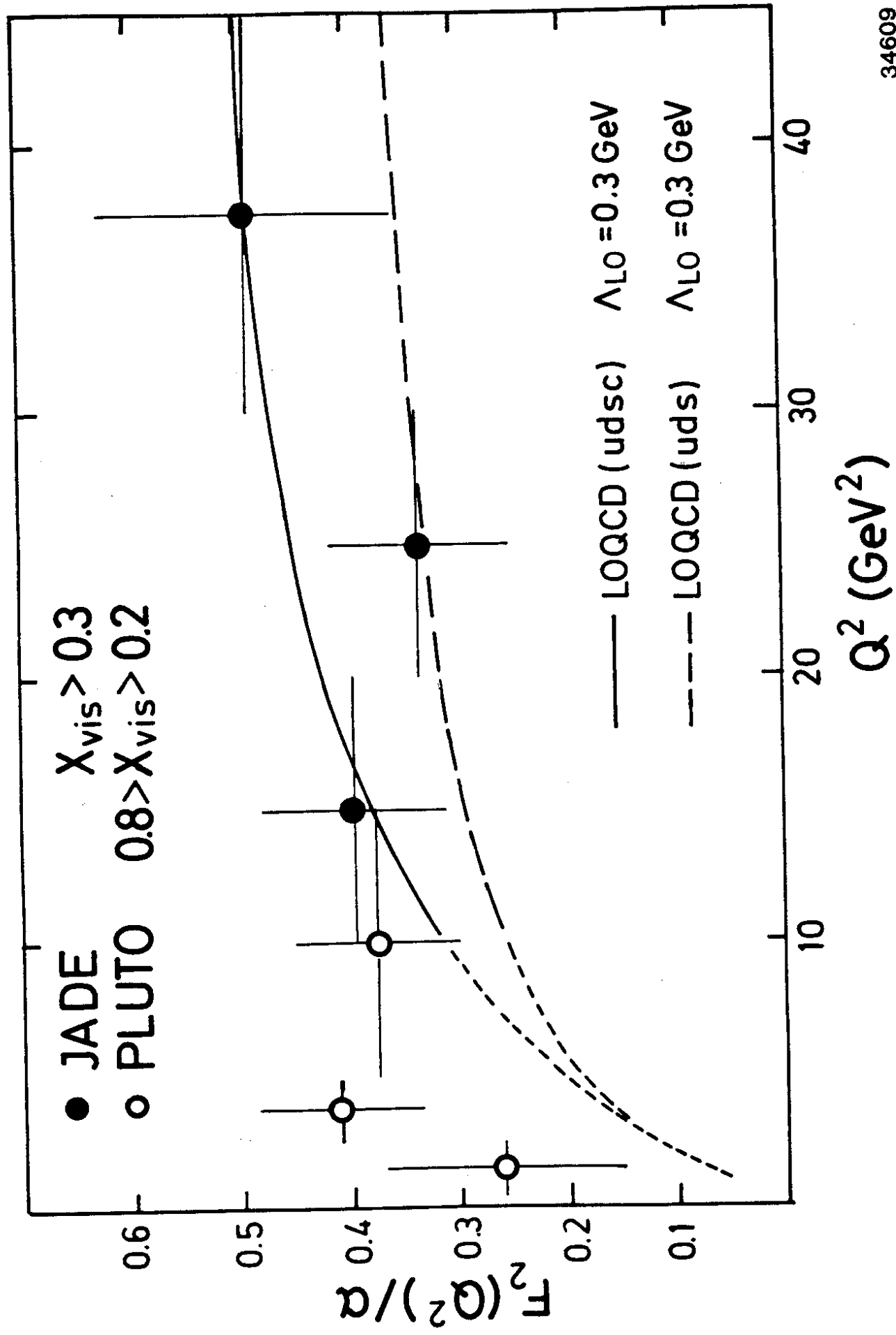


Fig. 2b



34605

Fig. 2c



34609

Fig. 3

